SANDIA REPORT
SAND2011-6453
Unclassified Unlimited Release
Printed September 2011

Detection of Embedded Radiation Sources Using Temporal Variation of Gamma Spectral Data

Isaac R. Shokair

Prepared by
Sandia National Laboratories
Albuquerque, New Mexico 87185 and Livermore, California 94550

Sandia National Laboratories is a multi-program laboratory managed and operated by Sandia Corporation, a wholly owned subsidiary of Lockheed Martin Corporation, for the U.S. Department of Energy's National Nuclear Security Administration under contract DE-AC04-94AL85000.

Sandia National Laboratories

Issued by Sandia National Laboratories, operated for the United States Department of Energy by Sandia Corporation.

NOTICE: This report was prepared as an account of work sponsored by an agency of the United States Government. Neither the United States Government, nor any agency thereof, nor any of their employees, nor any of their contractors, subcontractors, or their employees, make any warranty, express or implied, or assume any legal liability or responsibility for the accuracy, completeness, or usefulness of any information, apparatus, product, or process disclosed, or represent that its use would not infringe privately owned rights. Reference herein to any specific commercial product, process, or service by trade name, trademark, manufacturer, or otherwise, does not necessarily constitute or imply its endorsement, recommendation, or favoring by the United States Government, any agency thereof, or any of their contractors or subcontractors. The views and opinions expressed herein do not necessarily state or reflect those of the United States Government, any agency thereof, or any of their contractors.

SAND2011-6453
Unclassified Unlimited Release
Printed September 2011

Detection of Embedded Radiation Sources Using Temporal Variation of Gamma Spectral Data

Isaac R. Shokair
Exploratory Systems Technologies Department

Sandia National Laboratories
Mail Stop 9103
P. O. Box 0969
Livermore, CA 94551-0969

Abstract

Conventional full spectrum gamma spectroscopic analysis has the objective of quantitative identification of all the isotopes present in a measurement. For low energy resolution detectors, when photopeaks alone are not sufficient for complete isotopic identification, such analysis requires template spectra for all the isotopes present in the measurement. When many isotopes are present it is difficult to make the correct identification and this process often requires many trial solutions by highly skilled spectroscopists.

This report investigates the potential of a new analysis method which uses spatial/temporal information from multiple low energy resolution measurements to test the hypothesis of the presence of a target spectrum of interest in these measurements without the need to identify all the other isotopes present. This method is referred to as targeted principal component analysis (TPCA). For radiation portal monitor applications, multiple measurements of gamma spectra are taken at equally spaced time increments as a vehicle passes through the portal and the TPCA method is directly applicable to this type of measurement. In this report we describe the method and investigate its application to the problem of detection of a radioactive localized source that is embedded in a distributed source in the presence of an ambient background. Examples using simulated spectral measurements indicate that this method works very well and has the potential for automated analysis for RPM applications. This method is also expected to work well for isotopic detection in the presence of spectrally and spatially varying backgrounds as a result of vehicle-induced background suppression. Further work is needed to include effects of shielding, to understand detection limits, setting of thresholds, and to estimate false positive probability.

Acknowledgements

Support of this work by the Department of Homeland Security's Domestic Nuclear Detection Office through its Secondary Reachback Program is gratefully acknowledged. The author would also like to thank Chris Kunz, Kristin Hertz, Will Johnson, and Tim Tooman for useful discussions and comments, and Noel Nachtigal for his support of this work.

Sandia is a multi-program laboratory operated by Sandia Corporation, a Lockheed Martin Company, for the United States Department of Energy's National Nuclear Security Administration under contract DE-AC04-94AL85000.

Contents

I. Introduction **7**

II. Basis of Method for Detection of Embedded Sources **9**

III. Estimate of Statistical Variance **13**

IV. Application of TPCA for Detection of Embedded Sources **17**

Model Spectra 17
Temporal/Spatial Dependence of Simulated Measurements 18
Effect of Spectral Resolution 20
TPCA Analysis of Simulation Spectra – High SNR Test 21
TPCA Analysis of Simulation Spectra – Moderate SNR Test 25
Adding Adjacent Spectra 28
Detection by Direct Use of Measurements 29

V. Multiple Region Analysis **31**

VI. Detection of Multiple Isotope Sources **35**

Appendix A: Description of Generation of Principal Components **37**

Appendix B: Representation of Signals by Idealized Simple Sources **41**

References **43**

I. Introduction

Radiation Portal Monitors (RPMs), have been deployed at border crossings and other locations across the United States for the purpose of detection of illicit radioactive materials, with emphasis on special nuclear materials (SNM). These detectors measure gamma and neutron radiation as a vehicle passes through the portal, producing a series of spectral measurements for each vehicle. The RPM system alarms if a vehicle's profile exceeds a fraction of the background level and/or the energy spectrum has specific characteristics associated with SNM. Vehicles that result in alarms are usually routed for a more rigorous secondary inspection that includes additional measurements as well as imaging of the cargo in some cases.

The measured profiles for the majority of vehicles indicate the absence of radioactivity and show suppression of the ambient background as a result of shielding by vehicle structure and cargo. In a small fraction of vehicles, the measured profiles show the presence of radioactive sources that are mostly made up of naturally occurring radioactive materials (NORM), but also include other sources such as medical and industrial isotopes. Given the large volume of commerce, the total number of vehicles with radioactive material becomes significant. Since identification of the radiation source through manual inspection of the cargo is time consuming and manpower exhaustive, it is desirable to develop enhanced algorithms and analysis methods that improve the power of detecting illicit sources while reducing the false positive rate (i.e. the ability to distinguish benign and illicit sources of radiation with high confidence). The use of such algorithms in deployed systems would allow for reduction of alarm thresholds to increase sensitivity while improving throughput. The latter is accomplished by the ability to confidently detect and identify cargo with benign sources of radiation at the primary lane without the need to send a vehicle to secondary inspection. Previous studies have explored and demonstrated data transformation methods to differentiate NORM cargo from other isotopes[1-2].

With automated analysis algorithms, it is equally important to consider all realistic scenarios that could result in incorrect conclusions. This is especially important for extremely low probability events that can have major catastrophic consequences, such as terror related activity. One such scenario is that of transport of illicit radioactive materials embedded in NORM cargo in an attempt to conceal their radiation signal. A previous study of this type of scenario was conducted for low resolution polyvinyl toluene (PVT) detectors with only two energy channels[3]. This study used the spatial profile of total counts to detect potential embedded sources and then used the available spectral information to determine if the region containing the potential source is different spectrally in a statistically significant way from the remainder of the profile.

In this report we investigate the use of a novel spectral analysis method for detection of embedded sources for RPM applications with low energy resolution where photopeaks alone are not sufficient for isotopic identification. This method, referred to as Targeted Principal Component Analysis (TPCA), tests the hypothesis of the presence of a target isotope of interest without regard to other isotopes that are present in the measurement. This is accomplished using a form of data fusion of the spectral and spatial/temporal information. The requirement for this method to work is that the spatial profile for the target isotope of interest is different from other isotopes present in the measurement. Essentially, as is done in the subtraction of a constant

ambient background, this method allows for the subtraction of spatially varying backgrounds in a self-consistent and transparent way.

The method has a wide range of applicability for many spectral detection problems[4]. Because of its reliance on spatial contrast between different isotopes it is believed that this method is ideally suited for the problem of detection of embedded sources using low or medium energy resolution detectors since an embedded source is expected to have a much smaller extent than the other radioactive cargo containing it. This is the subject of this report.

In section II the method is described in some detail and in section III the method for variance estimation is described. Examples of detection of embedded sources and dependence on various parameters are described in section IV. The remainder of the report discusses some aspects of optimization and extension to more complex problems where the embedded source is made up of multiple isotopes.

This report provides an introductory description of the analysis and the examples considered are highly idealized and do not contain important physics effects such as shielding. Extension of this work to more realistic cases will be the subject of a future report.

II. Basis of Method for Detection of Embedded Sources

The Targetted Principal Component Analysis (TPCA) method has the advantage of exploiting spatial or temporal variations of multiple spectral measurements to test the hypothesis for the presence of a specific target isotope, when there are multiple unknown isotopes present in the measurements[(4)]. This method is ideally suited for Radiation Portal Monitor (RPM) applications for the problem of detection of a localized radiation source that is embedded in a distributed source. It is expected to work well for ASP-like detectors where multiple gamma spectra are collected at multiple time steps and might also be extendable to detectors with a small number of spectral bins such as the SAIC RPM-8 detectors.

The basis for the TPCA method was discussed in reference (4) and is repeated here for completeness in the context of the problem under consideration. In conventional spectral analysis, a measured spectrum is expressed in terms of signature (template) spectra and a confidence metric for target presence is estimated based on the calculated coefficient for the target signature and the goodness of fit using some optimization method such as least squares regression analysis. All isotopes present in the measurements need to be represented by template spectra in the analysis. In the TPCA approach, the opposite is done: the hypothesis target spectrum is represented as a linear combination of principal components or factors of measured spectra at multiple locations or times. With sufficient spectral differences between the target and other isotopes present in the measurements, this representation is possible when the target spectrum is present with a different spatial/temporal profile from the other isotopes. For this to be possible, without knowledge of spectra for all the non-target isotopes, the spatial or temporal variation needs to be subject to a constraint, expected to be satisfied for the case of embedded sources. The constraint and method are illustrated by use of the following simple example. Consider the case of a target with a known spectrum $\psi_t(E)$ and an unknown background with spectrum denoted by $\psi_b(E)$. Consider two measurements, $\psi_1(E)$ and $\psi_2(E)$ that contain both target and background isotopes. In the linear case the measured spectra can be written as:

$$\psi_1(E) = C_1\ \psi_t(E) + C_2\ \psi_b(E) \tag{1}$$

$$\psi_2(E) = C_3\ \psi_t(E) + C_4\ \psi_b(E) \tag{2}$$

For this trivial example the step of generation of principal component spectra can be bypassed and we can write the solution for the target spectrum $\psi_t(E)$ in terms of the measured spectra as:

$$\psi_t(E) = \frac{\left(C_4\ \psi_1(E) - C_2\ \psi_2(E)\right)}{\left(C_4\ C_1 - C_2\ C_3\right)} \tag{3}$$

The denominator in the above equation is the determinant of the coefficients and a solution exists for the non-singular case when $\frac{C_1}{C_3} \neq \frac{C_2}{C_4}$. This is precisely the variation requirement specified previously, that is, either target or background signal level varies between the two measurements such that the ratio is not constant. This shows that when the variation requirement is met, the

target spectrum can be expressed as a linear combination of the two measured spectra. Thus the hypothesis of target presence can be tested by a fit of the known target spectrum to the two measured spectra without any knowledge of the background spectrum. If the variation requirement is violated this fit will not be possible for the ideal noiseless case.

The above example can be extended to the case with N measurements containing target + (N-1) unknown background isotopes at varying concentrations. For large N the variation requirement remains simple, that is, between the different measurements the ratio of concentration of target to background isotopes varies. This constraint is clearly satisfied for the case of a localized source that is embedded in a distributed source in an ambient background which is the subject of this report. Two or more measurements with identical ratio of target to background concentration are considered identical in the sense of information content and thus can't be isolated.

For the general case of a target in the presence of other background isotopes, the measured spectra can be written as linear combinations of the target and background template spectra as:

$$M_i(E) = a_i\ T(E) + \sum_{\text{background, j}} b_{ij}\ B_j(E) \qquad i = 1,\ldots, N \tag{4}$$

where T is the target spectrum, B_j is the j-th background spectrum, and M_i is the i-th measured spectrum, all functions of the gamma energy E. Note that the target and background spectra may depend on shielding and detector effects. With some mixing of the target and background signals during measurements, linear independence between entities will be established as discussed in the above simplified example, and with this linear independence, the target spectrum can be written as a linear combination of the measurements, that is:

$$T(E) = \sum_{i=1}^{N} c_i\ M_i(\mathrm{E}) \tag{5}$$

When the number of measurements is large, principal component (PC) spectra can be used to limit the representation of the target spectrum to the physical variance of the measurements (assuming the higher order PCs mostly represent statistical noise):

$$T(E) \approx \sum_{i=1}^{N'} \alpha_i\ P_i(E) \qquad N' << N \tag{6}$$

where $P_i(E)$ denotes the i-th PC spectrum. The coefficients can then be estimated using Least Squares (LS) optimization of the reduced residual χ^2 which is given by:

$$\chi^2 = \frac{1}{(M_c - N')} \sum_{j=1}^{M_c} \frac{\left[T(E_j) - \sum_{i=1}^{N'} \alpha_i\ P_i(E_j) \right]^2}{\hat{\sigma}^2(E_j)} \tag{7}$$

where M_c is the number of energy channels and $\hat{\sigma}^2(E_j)$ is the estimated statistical variance for the j-th energy channel. This variance is due to statistical measurement noise and needs to be distinguished from physical variance between different measurements due differences between target and background spectra. The statistical variance estimate is considered in the next section. Note that $(M_c - N')$ is the number of degrees of freedom. Also note that N' in Eq. (6) needs to be significantly smaller than the dimension of the measurement space (number of energy channels) to insure that no false positives result from the effects of orthogonal noise components. By using principal component decomposition and for sufficiently high signal-to-noise ratio (SNR), the desire is to isolate the physical variance due to the target and background spectra in the low-order PCs, so that high-order PCs represent mostly measurement noise. Doing so, the linear combination given in Eq. (6) isolates the target from the backgrounds without any knowledge about the background spectra being required for the analysis. The specific method used to derive the PC spectra is discussed in Appendix A.

Depending on the measurement process and parameters, it is possible to increase the SNR by reducing the spectral resolution, i.e. summing multiple energy channels. However, sufficient discrimination between the target and background spectra (which includes the distributed source) has to be maintained including the effects of shielding and calibration drifts. Because of improved isolation of noise from physical spectral characteristics with decreased spectral resolution, it is possible that fewer PC spectra will be needed for isolation of the target spectrum. The tradeoffs between spectral resolution and the number of representation PC spectra will be the subject of a future optimization study. For most of the cases considered in this report, five PC spectra will be used.

For embedded localized sources the spatial extent of the target signal is expected to only cover a subset of the total vehicle length. For this situation, the larger the subset used to derive the PCs, the lower the overall contribution of the target to the PC spectra and thus the more likely that the target spectral information will be buried in higher order PCs and mixed with the noise. Therefore it is expected that there will be an optimum subset that should be used so that the target contribution is maximized while at the same time including the needed spatial/temporal variation to be able to isolate the target from the background clutter. Choice of the analysis region will be further discussed in section IV in this report.

III. Estimate of Statistical Variance

The reduced χ^2 residual given by equation (7) requires an estimate of the statistical variance. This residual is used for statistical evaluation of the target hypothesis. In conventional gamma spectral analysis when a measurement is represented by a linear combination of a number of template spectra, the variance can be estimated directly from the measurement since the counts are expected to follow Poisson statistics. For this case a good estimate of variance is obtained from the filtered spectrum on a channel by channel basis. The filtering reduces the effects of noise, especially for low counts, and attempts to approximate the true variance of the measurement. A filtering algorithm capable of handling large dynamic ranges is used for estimation of variance in the Gamma Detector Response and Analysis Software (GADRAS)[5-7].

For the TPCA method, the solution (fit to the target spectrum) is in the form of a linear combination of PC spectra, which are linear combinations derived from the measured spectra. The statistical variance in this case might not be correlated at all with the target spectrum since the clutter spectra (background and distributed source) are subtracted in the process of obtaining the solution. The variance also depends on the calculated coefficients which in turn depend on the variance through the optimization process. Therefore an iterative method can be used where an initial solution is obtained without variance weighting and then the estimated variance can be used in subsequent iterations to refine the solution until a self-consistent solution is obtained. In general convergence is expected to be rapid, but understanding and proving convergence requires further investigation of various test cases at varying SNR and will not be considered in this report.

Two methods of variance estimation were considered. The first method is based on the following simple procedure: 1- An initial fit of the target spectrum is obtained without variance weighting. 2- The calculated fit is polynomial smoothed (Savitzky-Golay filter) using parameters such that the physical features of the target spectrum are not significantly distorted (peak resolution of the detector can be used to guide the choice of filtering parameters). 3- Squared deviation between filtered and original fit spectrum is calculated. 4- The squared deviation is filtered and used as an estimate of variance.

The second and more formal method of variance estimation directly uses the measurement statistical variance. As discussed in the previous section, the TPCA method expresses the target spectrum as a linear combination of PC vectors. Since the PC vectors are themselves linear combinations of the measurements, it is possible to express the target spectrum as an overall linear combination of the measurements. Thus Eq. (6) can be written as:

$$T(E) \approx \sum_{i=1}^{N} \mu_i \; M_i(\mathrm{E}) \tag{8}$$

Equation (8) is similar but not identical to Eq. (5), and is based on the exact relationship between the PC vectors and the measurements as discussed in Appendix A. Given such a description, the overall variance of the fitted target spectrum can be written as:

$$\text{variance}\left[T(E)\right] \approx \sum_{i=1}^{N} (\mu_i)^2 \ \text{variance}\left[M_i(E)\right] \tag{9}$$

which applies at every energy channel E. Since the measurements are assumed to follow Poisson statistics, the variance of a measurement can be estimated in the normal way as the value of the filtered spectrum for each energy channel. It is also possible to co-add a number of spectra from adjacent measurements as a form of additional filtering if the physical variation between the adjacent measurements is not expected to be large.

The expression given in Eq. (9) does not include contribution to variance from the coefficients which is expected to result in small errors. Note that for each statistical realization of the set of measurements the derived PC vectors will be different and therefore the coefficients in Eq. (8) will have an associated variance. We will attempt to estimate the significance of this contribution to variance in future studies.

Now we turn to evaluation of the coefficients in Eq. (8). In appendix A, the PC vectors are expressed in terms of the measurement vectors by:

$$P_i = \sum_{k=1}^{N} \xi_{ki} \ M_k \tag{10}$$

Combining this with Eq. (6) we can write:

$$T \approx \sum_{i=1}^{N'} \alpha_i \left(\sum_{k=1}^{N} \xi_{ki} \ M_k \right) = \sum_{k=1}^{N} \left(\sum_{i=1}^{N'} \alpha_i \ \xi_{ki} \right) M_k \tag{11}$$

and

$$\mu_k = \sum_{i=1}^{N'} \alpha_i \ \xi_{ki} \qquad k = 1, \ldots, N \tag{12}$$

These coefficients are then used in Eq. (9) to obtain numerical estimates of variance which can be used in Eq. (7) to iteratively obtain a solution. The converged residual χ^2 is then used to compare the plausibility of different target hypotheses.

The above two methods of variance estimation were tested for a small number of cases and both resulted in reasonable values for the reduced χ^2 residual. However, additional testing is needed to understand the advantages and disadvantages of the two methods. For the analysis presented later in this report we will only consider the second method since it appears to have a sounder physical basis and only requires one filtering process. It should be noted however that even with a justifiable variance estimate, more detailed statistical analysis and justification is needed to conclude that the residual given by Eq. (7) possesses the same properties compared to classical linear least squares (LS) optimization. Such an analysis is beyond the scope of this report.

Regardless of the variance estimation method used, when measurement counts are zero for several adjacent channels, it is possible that the filtering will result in zero or negative variance for one or more channels. To avoid this singular behavior, a lower limit on the channel variance as a fraction of the average variance over all the channels is imposed. All channels below this limit are not used in the evaluation of the χ^2 residual. However, such channels are still used in evaluation of the PC spectra.

IV. Application of TPCA for Detection of Embedded Sources

In this section we present a simple example of the application of the TPCA method for detection of a localized source that is embedded in a distributed source in the presence of an ambient background. This is done in the context of an RPM measurement of a vehicle with multiple time samples. The combinations of isotopes used for the sources and background were chosen to generate sufficiently complex spectra for illustrative purposes only, and otherwise they have no application to any specific real measurement. For this analysis the effects of shielding and background suppression are not considered.

Model Spectra

For this test the localized source is ^{137}Cs and is embedded in a distributed source which is made up of a mixture of four isotopes (^{226}Ra, ^{232}U, ^{201}Tl, and ^{60}Co). The background spectrum is made up of two isotopes (^{40}K and ^{232}Th). The spectra for all the isotopes were generated using the GADRAS 1D model (spherical) for a NaI detector (GR-135) at a distance of 100 cm from the edge of the spherical source of 10 cm radius. The source shell is made of a material specified in GADRAS as "Cargo" with a density of 0.4 g/cm^3 with a specified activity of 10 μCi for each isotope (note the detected gamma counts for the isotopes can be significantly different because of differences in branching ratios and gamma energies). For isotopes with daughters, the resulting GADRAS spectra include contributions of decay of all daughter isotopes (20 years was used for the age in the GADRAS model). The baseline model spectra (noiseless) for the sources and background at the specified activity of 10 μCi for all isotopes are shown in the figure below.

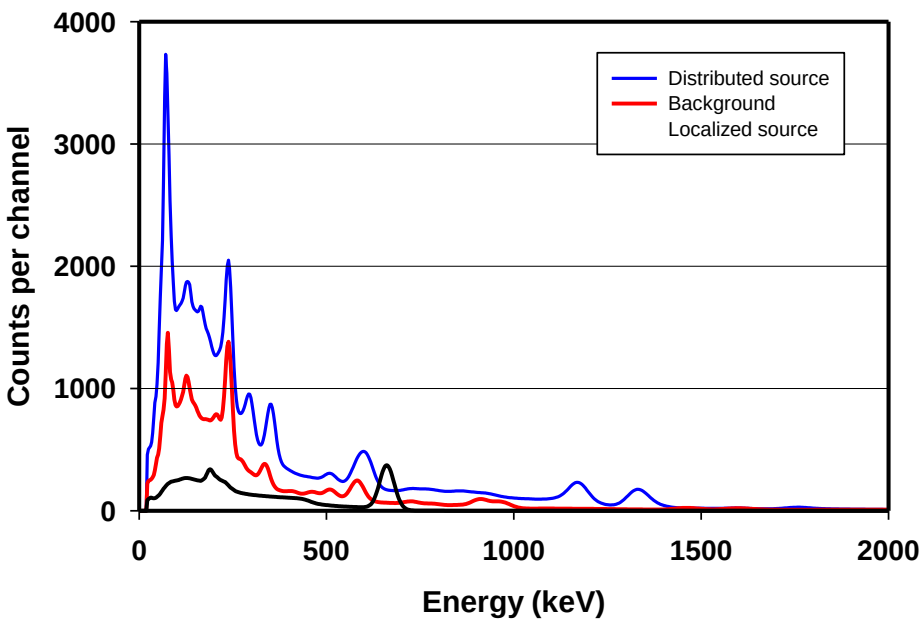

Figure 1. GADRAS model spectra for the sources and background. The distributed source spectrum is the sum over model spectra for ^{226}Ra, ^{232}U, ^{201}Tl, and ^{60}Co, each at 10 μCi. The background is sum over model spectra for ^{40}K and ^{232}Th, each at 10 μCi. The localized source is ^{137}Cs at 10 μCi. The detector used is a GR-135 at 100 cm distance from the source (sources are modeled as 10 cm radius spheres with uniformly distributed isotopes).

Temporal/Spatial Dependence of Simulated Measurements

The situation under consideration here is that of a vehicle passing through a radiation portal monitor. The radioactive cargo is distributed along the length of the vehicle and at some location an additional localized source is embedded in the cargo. For this analysis we use idealized line and point sources to model the spatial distribution of the distributed and embedded sources. These simple models have been used in previous analysis[(3)] and with proper choice of parameters can result in profiles that match measured profiles very well. The description of the source models is given in appendix B for completeness. It should be noted that many other models have been used and most can generate similar profiles by proper choice of the source parameters.

The spatial distributions of the sources result in a time dependent measured signal as the vehicle passes through the portal. For the point, *P*, and distributed, *D*, sources the profiles are given by:

$$f_P(z) = A_0 \left[\frac{R_0^2}{R_0^2 + (z - z_o)^2} \right]^{3/2} \tag{13}$$

$$f_D(z) = \alpha_0 \left\{ \frac{z - z_o + \Delta}{\left[R_o{}^2 + (z - z_o + \Delta)^2 \right]^{1/2}} - \frac{z - z_o - \Delta}{\left[R_o{}^2 + (z - z_o - \Delta)^2 \right]^{1/2}} \right\} \tag{14}$$

$$f_D(z = z_0) = \frac{2\,\alpha_0\,\Delta}{\left[R_0^2 + \Delta^2 \right]^{1/2}} \equiv A_0 \tag{15}$$

where $(z - z_0)$ is the distance from the source center to the center of the detector along the direction of vehicle motion. The other source parameters are defined in appendix B. Figure (2) shows sample profiles for typical source parameters.

The simulated measured spectrum as a function of time sample (or position along direction of vehicle motion) is given by the profile-modulated model spectra as follows:

$$S(z, E) = C_p\, S_P(E)\; f_P(z) + C_D\, S_D(E)\; f_D(z) + C_B\, S_B(E) \tag{16}$$

where the profile modulation functions $f_P(z)$ and $f_D(z)$ are given by equations (13) and (14). The spectra $S_P(E)$, $S_D(E)$, and $S_B(E)$ are the point source, distributed source, and background spectra respectively that are shown in figure (1) above. The coefficients C_P, C_D, and C_B will be used to scale the counts to realistic levels for the detection analysis. After the scale factors are applied, Poisson statistics are applied to the simulation spectra at all *z* and *E* values.

Figure (3) shows the total counts profile (summed over all energy channels) for a simulation with scale factors: $C_P = 0.02$, $C_D = 0.01$, and $C_B = 0.01$. A total of 160 time samples are used. The simulated spectra represent measurements at different time samples as the vehicle passes through the portal. At the time sample of maximum counts (time sample 111), the simulated spectrum is

shown in figure (4). As noted earlier the simulated spectra do not include effects of shielding or background suppression. The width of each time sample is assumed to be 0.1 seconds for comparison to RPM measurements.

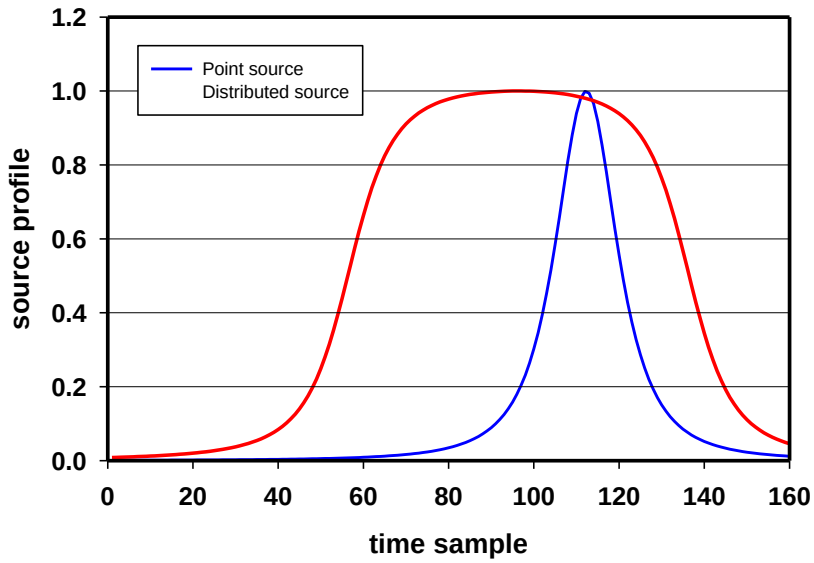

Figure 2. Model profiles for point and distributed sources. All spatial quantities are normalized to the overall vehicle length and the first and last time samples correspond to the entry and exit of the vehicle from the portal respectively. A total of 160 time samples are used. The normalized source parameters are: Point source: $z_o = 0.7$, $R_o = 0.07$. Distributed source: $z_o = 0.6$, $R_o = 0.07$, $\Delta = 0.25$.

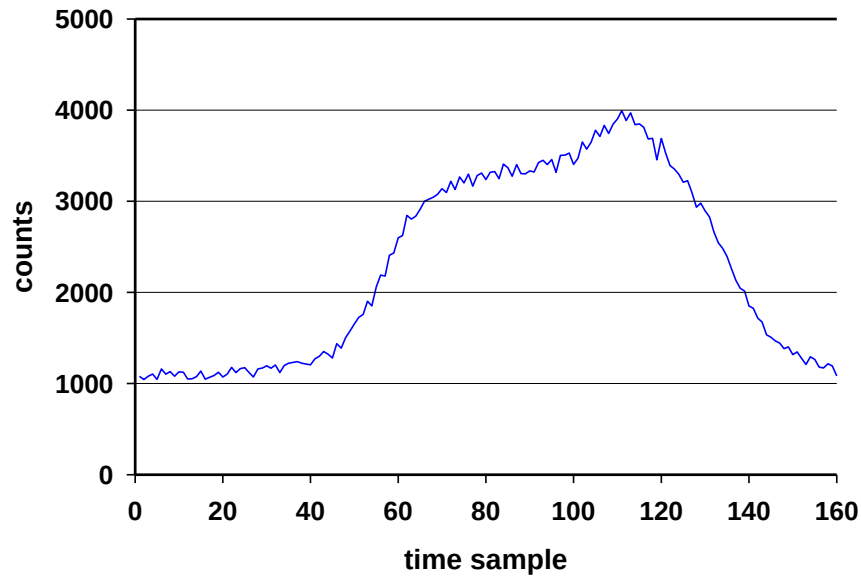

Figure 3. The total counts profile as a function of time sample. The sources and background spectra are scaled by the factors: $C_P = 0.02$, $C_D = 0.01$, and $C_B = 0.01$. The source geometric parameters are the same as in figure (2).

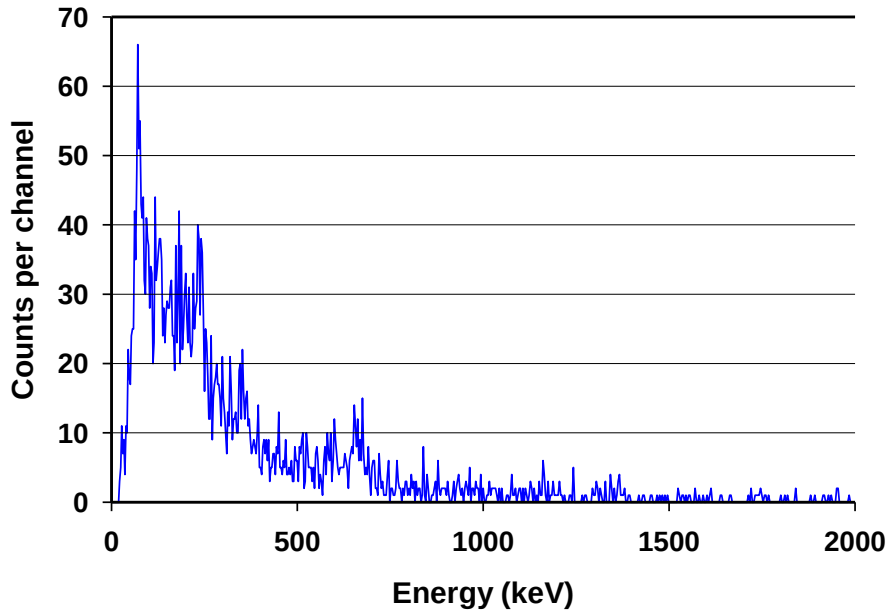

Figure 4. Simulated spectrum for the time sample with maximum total counts (time sample 111). All parameters are the same as in figure (3).

Effect of Spectral Resolution

As discussed in reference (2), for the TPCA method to work efficiently, it is important that the principal component (PC) spectra used in the analysis reflect the true physical variance present in the measurements with the effect of statistical noise minimized as much as possible. When the signal-to-noise ratio (SNR) of the measurements is sufficiently low, the resulting low order PC spectra can become more a reflection of statistical noise rather than physical spectral variation, clearly a situation that needs to be avoided. For the same sources and measurements, the SNR can be increased by co-adding spectra and/or summing counts for multiple spectral channels (referred to here as reducing spectral resolution). Both of these techniques can be used with the constraints that spatial/temporal variation and discriminating spectral features are not washed out in the process.

Another important consideration in optimization of the spectral resolution used in analysis is to consider possible alternate hypotheses for the target spectrum. Reduction of the spectral resolution can result in reduction of the orthogonal component between the target spectrum of interest and other non-target isotopes possibly leading to false positives. Thus it is important to consider possible interferents when optimizing the analysis parameters.

In this report we will consider the effect of changing the spectral resolution from 1024 to 256 and 128 channels by adding counts in adjacent channels. The effect of this reduction on discrimination capability can be quantified by the length of the orthogonal component between normalized spectra. For normalized spectra denoted by the vectors $\vec{S}_1$ and $\vec{S}_2$ (vectors of counts in each channel normalized to a length of 1) this length is:

$$l = \left\{1 - p^2\right\}^{1/2} \qquad p = \vec{S}_1 \bullet \vec{S}_2 \tag{17}$$

where the dot product is defined in the usual way for a finite dimensional space, that is, *p* denotes the parallel component between the two spectra. Table 1 shows the lengths of the orthogonal components between the source spectra for different resolutions. The loss of discrimination capability is minimal in going from 1024 to 128 channels for these sources. However, the results can be significantly different for other source isotopes, if other alternate hypotheses spectra are used, or spectral distortion due to shielding is significant.

Table 1. Orthogonal length between spectra for different spectral resolutions.

Spectral resolution (channels)	Target & distributed source	Target & background	Distributed source & background
1024	0.55	0.53	0.23
256	0.55	0.52	0.23
128	0.53	0.51	0.21

TPCA Analysis of Simulation Spectra – High SNR Test

The TPCA method was applied to the above simulation spectra for detection of the ^{137}Cs localized source without using any knowledge regarding the other isotopes present in the distributed source or the background. All the time sample measurements were used to derive the PC spectra and then LS optimization was applied using the ^{137}Cs target spectrum to determine the coefficients that minimize the χ^2 residual in equation (7).

For the first test, to illustrate the method and also as a check on the computer software used for the analysis, a high SNR case with scale factors C_P = 2.0, C_D = 1.0, and C_B = 1.0 was considered. The SNR for this test should be a factor of 10 higher than shown in figures (3 - 4). For these scale factors the results of application of the TPCA method with 5 PC spectra are shown in figures (5 - 7) for the first set of simulated measurements made up of 160 time samples. A total of 100 independent statistical sets were processed to estimate the properties of the resulting distribution of residuals. The average and standard deviation of the resulting reduced χ^2 residual are 0.9982 and 0.0054 respectively for the ^{137}Cs target hypothesis. For the variance estimate 4 iterations were used for each case (for these parameters one test showed that convergence is attained after 3 iterations) and the channels used in the LS fit were limited to those with variance larger than 0.0001 times the average to avoid singular behavior as discussed earlier. If the variance lower limit factor is changed from 0.0001 to 0.001, the average residual is 0.9972 and the standard deviation is 0.0055 for the same set of 100 simulations. This indicates that the lower limit used is adequate and has no effect on the resulting solution.

Figures (6 - 7) clearly show that for this high SNR case the first 3 PC spectra contain almost all the physical variance due to the localized source, distributed source, and background spectra while all other PC spectra are due to noise. When the simulations were run without including Poisson noise, only three eigenvalues have non-zero values and the fit to the target spectrum is perfect as expected (residual is identically equal to zero). As noted earlier, for the noiseless case, the three PCs correspond to orthogonal linear combinations of the localized source, distributed source, and background spectra. Note that the vertical scale in figure (6) is a result of using a covariance matrix that is not normalized to the number of measurements.

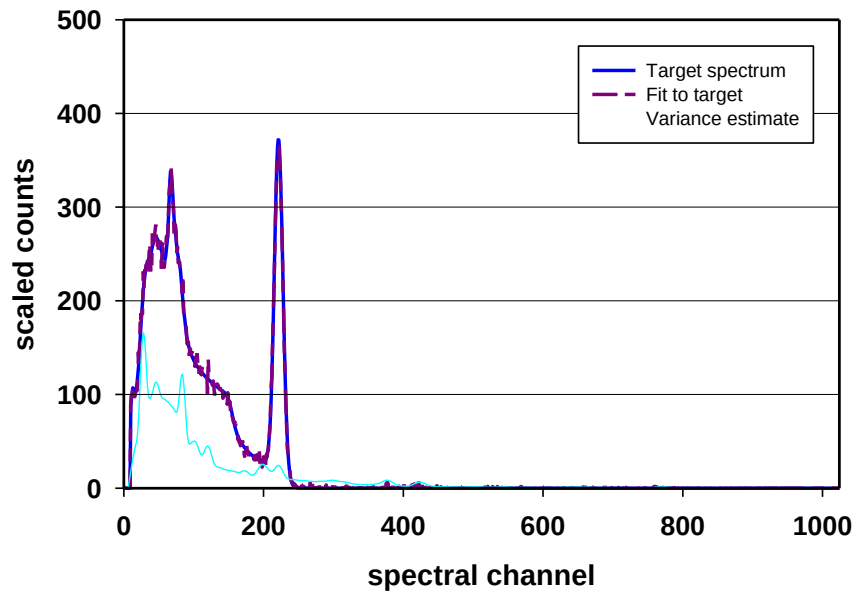

Figure 5. Target spectrum and fit using 5 PC spectra for a case with high SNR and 1024 energy channels. Also shown is the estimated variance. The scale factors used are: C_P = 2.0, C_D =1.0, and C_B = 1.0. The average reduced residual is χ^2 = 0.9982 for 100 statistical cases and using 4 iterations for the variance estimate. Note the shape of the variance profile is consistent with measured spectra and not necessarily the hypothesis target spectrum.

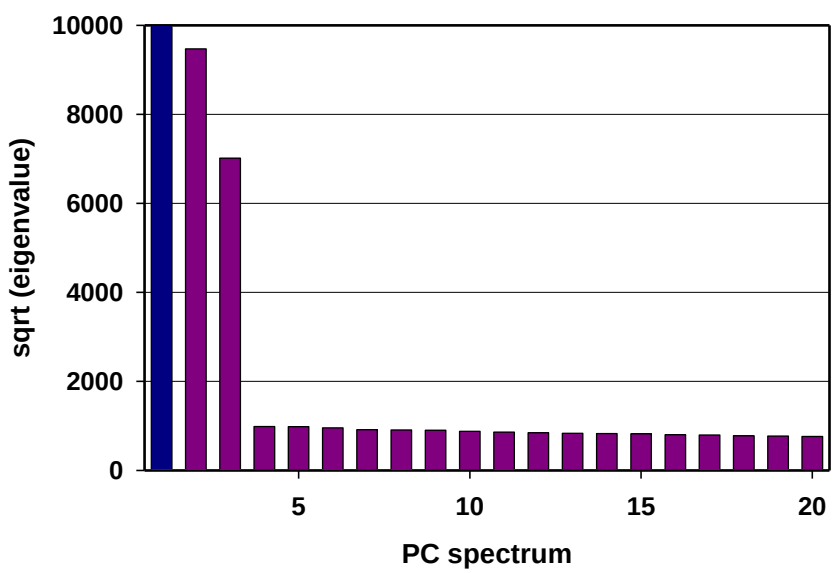

Figure 6. The first 20 eigenvalues in descending order for the PC spectra for simulations in figure 5. The first eigenvalue represents the mean of all the measurements used in obtaining the PC spectral vectors and is very large (off scale). The next two eigenvalues represent the remaining variance due to spectral differences between the localized source, distributed source, and background. All other eigenvalues (up to 160) mostly represent noise contributions. If Poisson noise is turned off in the simulations only three eigenvalues are non-zero. Note that in the PCA the covariance matrix is evaluated about the origin rather than the mean spectrum.

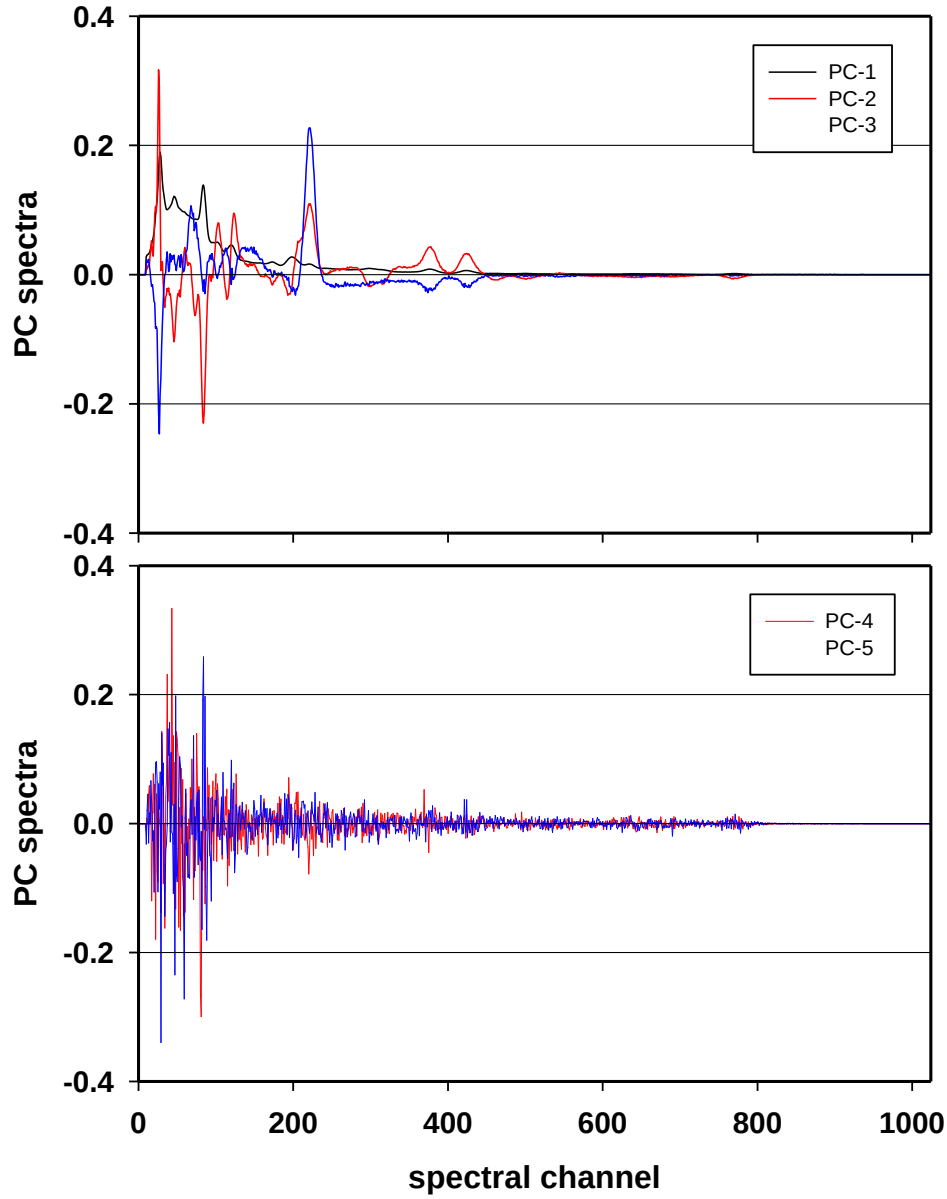

Figure 7. The first 5 PC spectra using all 160 simulated measurements in the time profile. It is clear for this high SNR case that the first 3 PC spectra contain almost all the physical variance due to the spectra for the localized source, distributed source, and background while all other higher order PC spectra are due to noise.

An important consideration in the analysis is the nature of the resulting distribution of the reduced residual values. Figure (8) shows a comparison between the classic χ^2 distribution (mean value of 1.0) and the distribution of reduced χ^2 values resulting from 10,000 statistically independent simulation sets for the same high SNR parameters used above (mean value of 1.05). Only the number of channels was reduced to 256 to reduce CPU time. Even though the

distributions are similar, they are not identical. The reason for the difference is not completely understood at the present time, but likely can be attributed to the spectral filtering algorithm that is used for estimation of variance (4-th degree and 21 samples centered polynomial filtering which was used for this test). An additional factor could be the ignored terms in the variance estimate discussed in the previous section. Simulations with a factor of 10 higher signal levels for all sources resulted in a nearly identical distribution. Further analysis is required to understand the differences between these distributions.

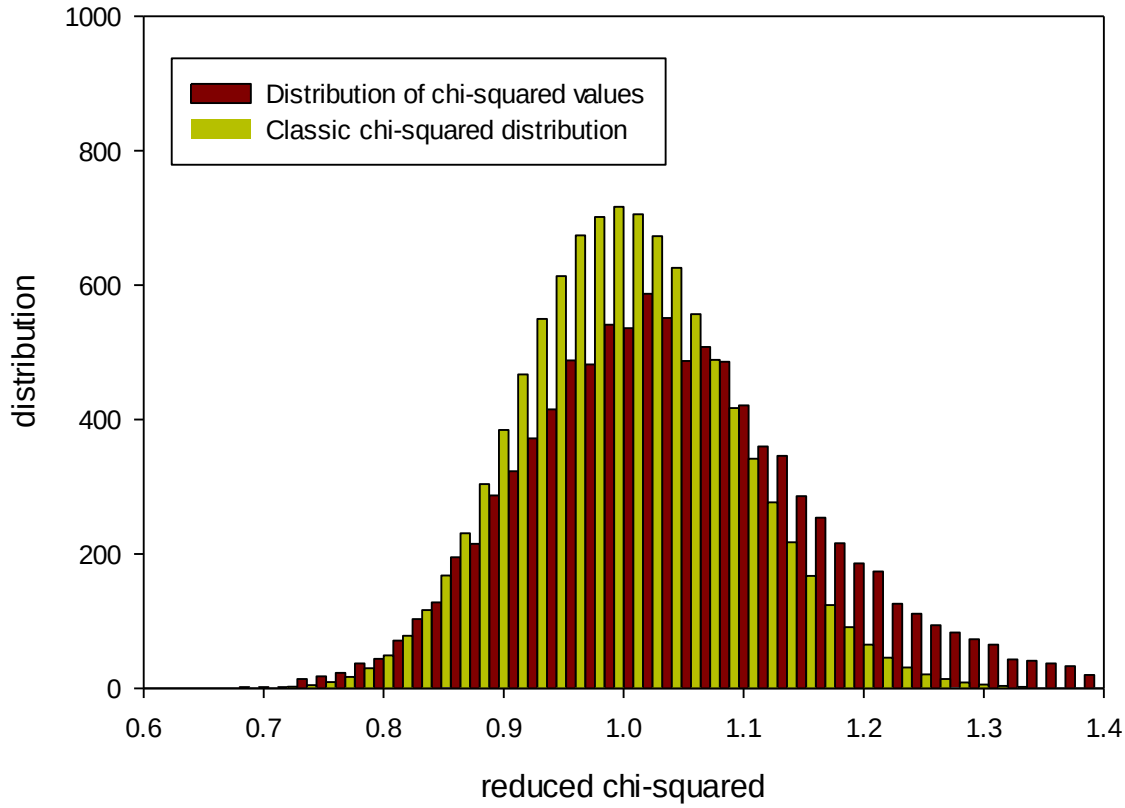

Figure 8. Comparison of the classic χ^2 distribution and distribution of reduced χ^2 residuals from 10,000 simulation sets for the same parameters as in figure (5), only the number of channels is reduced to 256. The number of degrees of freedom is 251 (256 channels minus 5 adjustable coefficients for the 5 PC spectra). The mean value of the reduced residual is 1.05.

Another simple but very important test is that of a false positive, that is, with the target scale factor C_P = 0.0 in the simulated measurements. Using identical parameters as used for the previous example, the average residual is 1054.3 and the standard deviation is 1923.6 for 100 simulations. The minimum residual is 138.6 which is extremely large and clearly indicates that the target isotope spectrum is not present at a statistically significant level in the simulated measurements. Thus the probability of a false positive is very small for the considered signal levels. The result of the LS fit from the first simulation is shown in figure (9). This analysis can also be extended to estimate an upper limit on the target signal that could be present with the other sources. This type of analysis is beyond the scope of this report and might be considered in a future study of detection limits for the TPCA method.

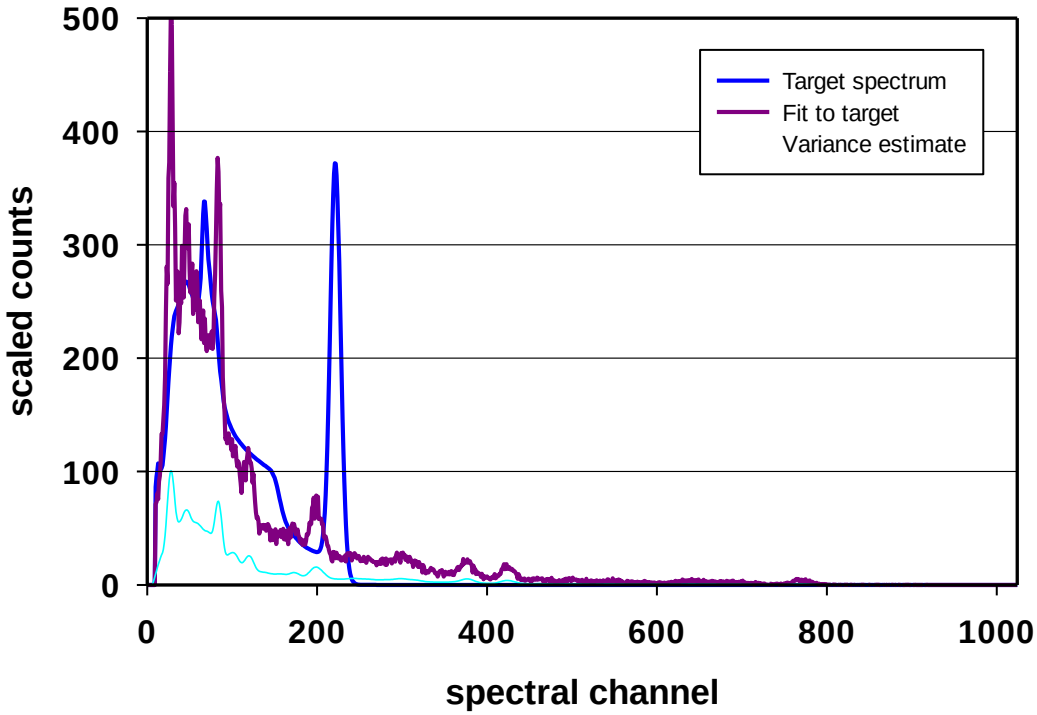

Figure 9. Target spectrum and fit using 5 PC spectra for simulations without target. The scale factors for the simulation spectra are: C_P = 0.0, C_D = 1.0, and C_B = 1.0. All other parameters are the same as in figure (5). The reduced residual for the case shown is χ^2 = 322.0 which is very large and indicates that the target hypothesis is highly improbable.

TPCA Analysis of Simulation Spectra – Moderate SNR Test

In this section we consider simulations with more realistic counts for the source spectra used previously. This analysis uses scale factors of C_P = 0.02, C_D = 0.01, and C_B = 0.01. At these values of the scale factors the counts are of the order of observed counts for real RPM measurements. This is seen in the total counts profile in figure (3) where it is assumed that each time sample has duration of 0.1 seconds as in actual RPMs.

The TPCA analysis was carried out using the first five PC spectra and the results are shown in figure (10) for three spectral resolutions for the ^{137}Cs target. Ranges of values of the reduced residuals are given in table 2 below.

Table 2. Range of values of reduced residuals

Spectral resolution (channels)	Mean χ^2	Standard Deviation	Minimum χ^2	Maximum χ^2
1024	3.34	0.71	2.09	6.87
256	1.74	0.25	1.20	2.35
128	1.62	0.32	0.91	3.14

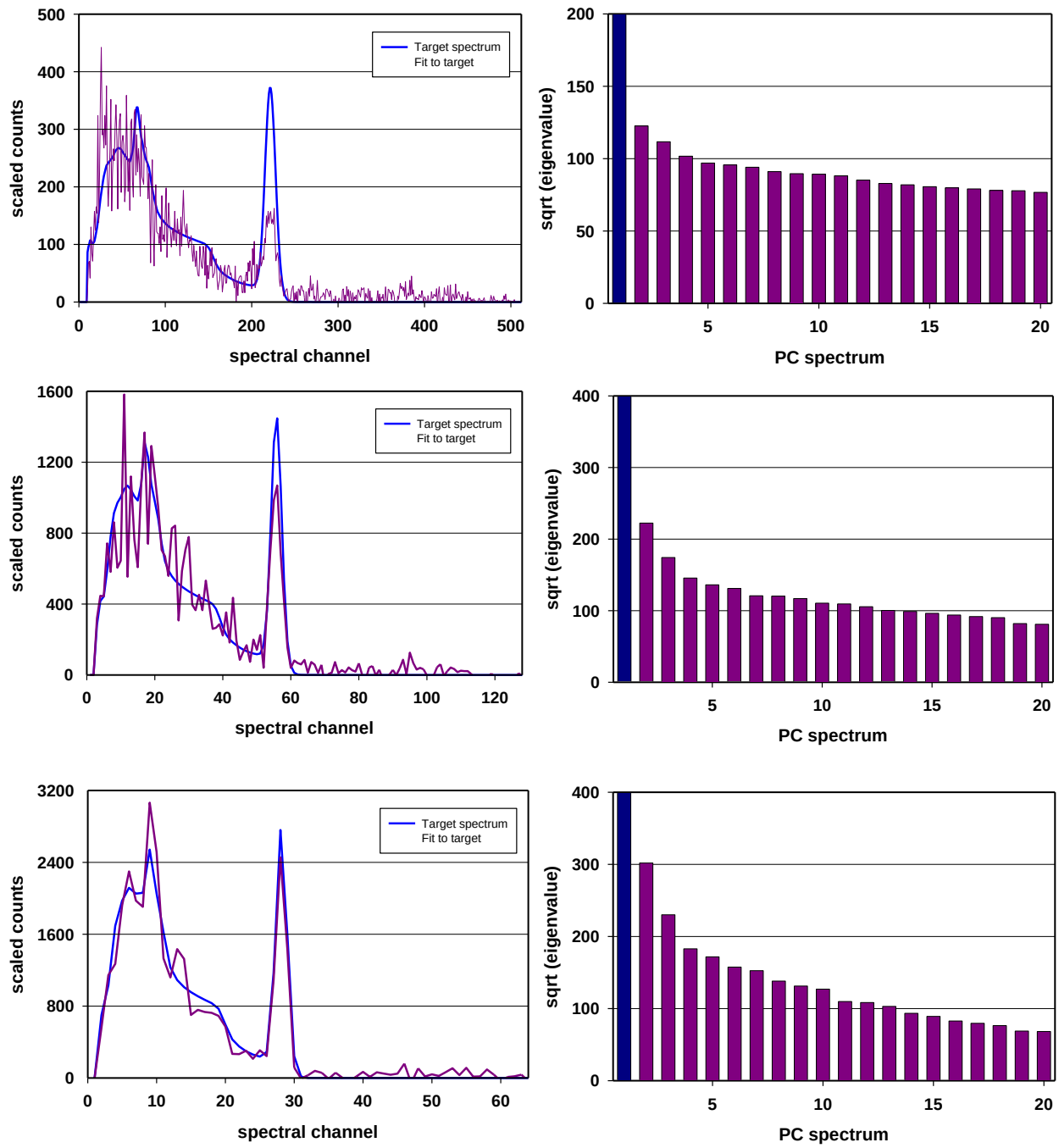

Figure 10. Results of application of the TPCA method for the ^{137}Cs target spectrum for different spectral resolutions. For all cases the first 5 PC spectra were used in the analysis. Only half the spectral channels are shown in the plots for clarity. The plots on the right show the first 20 eigenvalues – the first eigenvalue in dark blue is off the scale. Top: 1024 channels (χ^2 = 3.38), Middle: 256 channels (χ^2 = 2.02), Bottom: 128 channels (χ^2 = 1.41). The results are for the first simulation set out of a total of 100 that were run.

For all three spectral resolutions the same filtering parameters were used in the variance estimates (4-th degree polynomial smoothing with 21 samples). These filtering parameters are not necessarily optimal for any of the three cases and are likely the cause of the large residuals for the case with 128 channels. Further work is needed to obtain the proper estimate of variance for different spectral resolutions.

Even at the lowest spectral resolution, the eigenvalue plots indicate that the effect of noise is large and it is possible that five PC spectra are not sufficient to span the physical variance in the measurements and possibly lead to the larger than expected χ^2 residuals. To test this hypothesis we repeated the analysis for the 128 channel case using 10 PC spectra. The results are shown in figure (11). For this case the average $\chi^2 = 1.29$ and its standard deviation is 0.24 for 100 sets of simulations. The maximum residual is 1.88. This improvement clearly shows that the additional PC spectra contain physical variance in addition to a noise component. The relationship between spectral resolution and number of needed PC spectra will be the subject of a future optimization study for this detection method.

With additional PC spectra it is important to insure that the probability of false positives does not increase to unacceptable levels. For the same parameters as the above simulations, but without the target present, the average χ^2 is 52.1 and its standard deviation is 24.5 for 100 sets of simulations. The minimum residual is $\chi^2 = 19.8$ indicating no significant increase in the false positive rate.

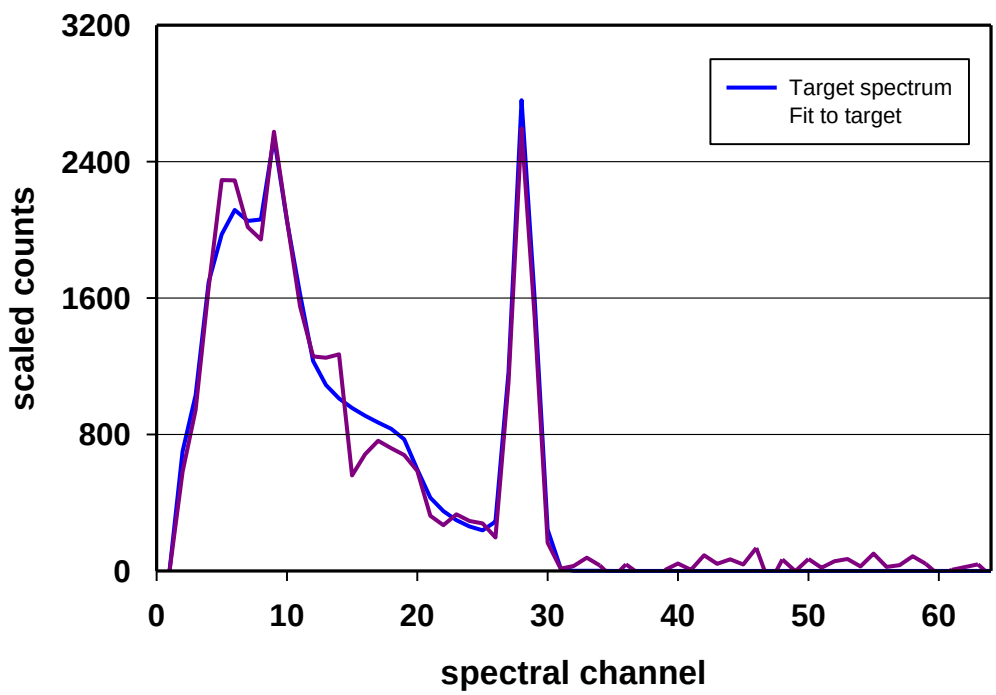

Figure 11. Results of application of the TPCA method for the ^{137}Cs target spectrum using 10 PC spectra and 128 spectral channels. The residual for this case is $\chi^2 = 1.24$.

The results considered in this section for an example with moderate SNR and large clutter (distributed source + ambient background) relative to the source of interest illustrate the usefulness of this method for detection of embedded sources using automated analysis. There are many possible techniques for optimization of the method to improve detection limits. We will consider a couple of such techniques in the following sections, but considerable further work is needed to fully establish the range of applicability of the method.

Adding Adjacent Spectra

For the problem under consideration and depending on the total number of time samples in an RPM measurement, it is possible for the localized source signal to extend over many samples. Because of the deleterious effect of noise on the calculated PC spectra, it is beneficial to co-add spectra from adjacent time samples when such addition does not adversely affect the variation requirement for the TPCA method. For the simulated measurements used in this report (see figure 2), the localized source signal extends over roughly 25 samples. Therefore we should be able to co-add spectra for groups of several adjacent time samples and still maintain a high degree of contrast between the localized source and the other sources while reducing the effect of noise. This process should improve isolation of physical variance from noise in the low order PC spectral vectors.

The results of co-adding 5 spectra are shown in figure (12) for two spectral resolutions. The eigenvalue plots show significantly improved separation between the first three PCs and the others. There is also significant improvement in the fit to the target spectrum as seen in the residuals (256 channels: average $\chi^2 = 1.26$ and standard deviation = 0.15. 128 channels: average $\chi^2 = 1.08$ and standard deviation = 0.19).

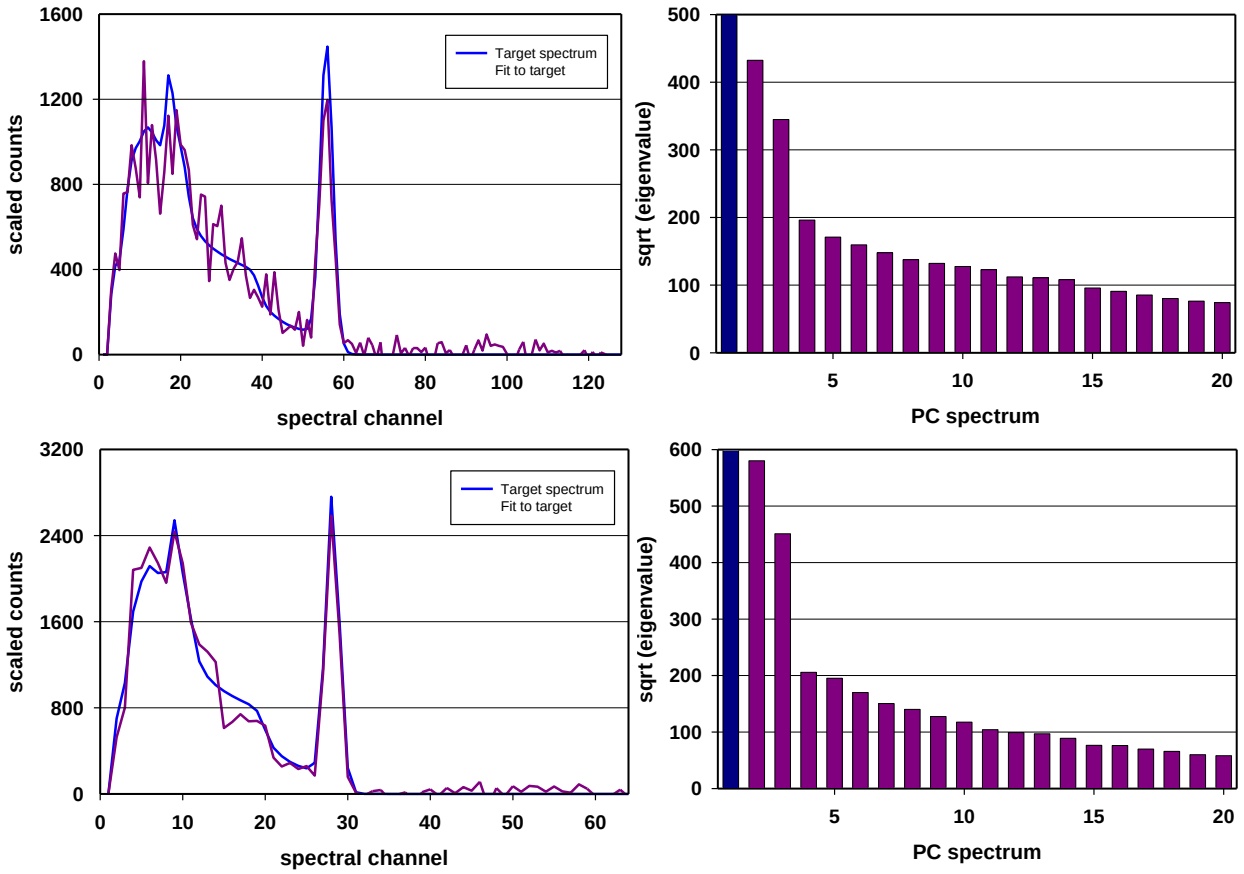

Figure 12. Results of application of the TPCA method for the ^{137}Cs target spectrum using 5 PCs. Each 5 simulated time sample spectra were added before application of the PCA. The residuals for these two cases are: top: χ^2 = 1.4 (256 channels) and bottom: 1.02 (128 channels).

Detection by Direct Use of Measurements

For the problem of detection of embedded sources for a specific detection system and concept of operations, the spatial extent of the source signal is somewhat known and can be bounded. This was the case for the simulations considered earlier. In such cases adjacent measurements can be added to form a small number of summed measurements which contain the spatial/temporal variation information required to enable isolation of the spectrum of the target of interest. In such cases, when the number of summed measurements is small, it is possible to bypass the PCA step and use the summed spectra directly instead of the PC spectra. This is considerably easier and also has the advantage of retaining spectral information that could be lost in higher order PC spectra not included in the solution. This is particularly important for low SNR cases.

For the example considered previously and using 5 overall spectra (each 32 time sample spectra were co-added), the results are shown in the table 3 below. As expected this shows some improvement over using PC spectra due to fuller use of the physical variance.

Table 3. Range of values of reduced residuals

Spectral resolution (channels)	Mean χ^2	Standard Deviation	Minimum χ^2	Maximum χ^2
1024	2.39	0.20	1.85	2.99
256	1.32	0.18	0.94	1.78
128	1.10	0.19	0.76	1.60

Other Geometries

The example discussed in the previous section dealt with a localized source that is embedded in a wide distributed source. The same method is expected to work as well for other source geometries such as multiple adjacent localized sources. The only requirement is that the target of interest must have a different spatial profile from the other clutter sources that are present so that its spectrum can be isolated from the others.

V. Multiple Region Analysis

In the previous section all simulated measurements that make up the vehicle profile were used in calculation of the principal component spectra that were then used in fitting the target spectrum which represents the localized embedded source. This is certainly not the optimal method for detection of the localized source. In some sense, obtaining this fit is equivalent to subtraction of the integrated (summed over time samples) background and distributed source spectra from the total spectrum if these two spectra were known. Thus the noise in the total spectrum is reflected in the fit for the target. Since the embedded source signal extends over a subset of the total vehicle length, it is useful to limit the analysis region to a subset of the total measurements that includes most of the rise and fall of the embedded source (to maintain the variation requirement), but excludes other measurements that do not contain significant embedded source signal in order to maximize the SNR of the source. However, the source location is one of the unknowns that needs to be determined by automated analysis.

In some instances the profile of total counts can be used to infer information on location and extent of a potential embedded localized source[(3)]. However, this might not work in all cases especially for low SNR. Since the spatial extent of a small source can be estimated (extent is smaller for shielded sources) and a specific target spectrum is being sought, it is possible to define a metric that provides information on the likelihood of target presence and use the region that maximizes this metric. An example of such a metric is the parallel component of the measured spectrum in a region to the target spectrum (see equation 17). The moving summed spectrum over the anticipated extent of the source and its parallel component to the target spectrum can be calculated as a function of time sample. The region with maximum parallel component is then the most likely to contain the target and can be used for application of TPCA. This method requires further development and testing and will not be considered in this report.

Another method considered here is to apply TPCA over multiple overlapping regions as shown in the illustration in figure (13). The extent of each region is of the order of the anticipated extent of the source signal. This method has the advantage that all time samples are tested for target presence.

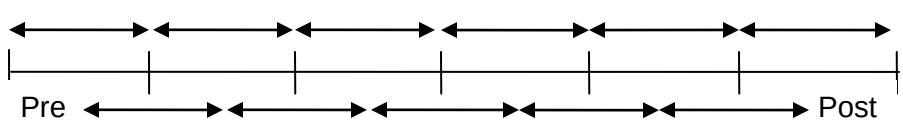

Figure 13. Illustration of overlapping regions to be used for analysis. The extent of the arrow defines the analysis samples for a region which should be wide enough to include most of the signal rise and fall for the localized source. For actual measurements pre- and post-samples do not need to be analyzed.

For multiple region analysis there are two quantities that need to be maximized for optimal detection of a localized embedded source with unknown location. First, the width of the analysis region or region of interest (ROI) needs to be chosen so that the target signal-to-noise ratio (TSNR) is maximized. Second, the signal contrast or variation between the localized source and other sources needs to be maximized.

Region Width:
For the localized source model given by equation (13) and for the limiting case when the distributed source and background can be approximated as constant over the ROI, the scaling of the TSNR can be approximated by the expression:

$$TSNR = \frac{\text{total target signal}}{\text{noise}} \propto \frac{\int_{z_1}^{z_2} dz \left[\frac{R_0^2}{R_0^2 + (z - z_o)^2} \right]^{3/2}}{\sqrt{(z_2 - z_1)}}$$

$$\propto \frac{R_0}{\sqrt{(z_2 - z_1)}} \int_{(z_1 - z_0)/R_0}^{(z_2 - z_0)/R_0} du \frac{1}{\left[1 + u^2\right]^{3/2}} \tag{18}$$

$$= \frac{R_0}{\sqrt{(z_2 - z_1)}} \left\{ \frac{u}{\sqrt{1 + u^2}} \Bigg|_{(z_1 - z_0)/R_0}^{(z_2 - z_0)/R_0} \right\}$$

where z_2 and z_1 denote the boundaries of the ROI. In equation (18) we made the additional assumption that the localized source amplitude is sufficiently small so that its contribution to overall noise can be neglected. Thus the noise which is proportional to the square root of the total signal in the ROI is approximately proportional to the width of the ROI. When the source is centered in the ROI we obtain:

$$TSNR \propto \frac{1}{\sqrt{\Delta}} \left(\frac{\Delta}{\sqrt{1 + \Delta^2 / 4}} \right), \qquad \Delta = \left(\frac{z_2 - z_1}{R_0} \right) \tag{19}$$

The RHS of equation (19) has a maximum value of 1.0 for $\Delta = 2.0$. This is the optimum width of the ROI for maximizing the TSNR for the source model used (when the source is centered). The maximum of equation (19) is somewhat shallow with a value of 0.9 for the RHS when $\Delta = 1.0$.

The other quantity to consider is the variation in source signal over the ROI which provides the contrast between the target and the other sources. This can be written as:

$$\Delta f_p = A_0 \left\{ 1 - \left[\frac{1}{1 + (Z_e - z_o)^2 / R_0^2} \right]^{3/2} \right\} \tag{20}$$

where Z_e is the edge (either left or right) of the ROI. This quantity increases with increasing region width. When the source is located at the center of the ROI Δf_p = 0.83, 0.65, and 0.28 for Δ = 3.0, 2.0, and 1.0 respectively. When the source is off center the contrast factor Δf_p increases for the side with the larger signal. However, even though we understand the requirement for having sufficient variation, it is not clear at this point what the optimum variation is and its effect

on the TPCA solution. For now we consider a value of $\Delta = 2.0$ to be reasonable for both TSNR and target signal variation.

Region Overlap:
Once the region width is chosen, the next issue to be considered is the amount of overlap between multiple regions for independent analysis. This is required since the source location is not known a priori. The safest and most optimal choice for overlap is to consider all possible regions, that is, advancing regions by a single time sample. This however is not practical from a computational point of view and is also not necessary. What is necessary is to maintain sufficient TSNR and target signal variation regardless of the source location.

As was discussed the contrast Δf_p increases for the side of a region with the larger signal as the source is moved from the center. This increase continues until the source maximum moves outside the region. If the next region has any overlap with the previous, the contrast Δf_p is then picked up by this new region. Thus it seems that the main issue for overlap is maintaining a reasonable value for the TSNR.

For two overlapping regions, the smallest TSNR (with all the assumptions and approximations that were discussed above) occurs when the source is located at the center of the overlap segment of the two regions. This is also the point at which the TSNR is equal for the two regions and can be referred to as the transition point. From equation (18) the TSNR for the region extending from z_1 to z_2 (all quantities are normalized to R_0) is given by:

$$TSNR \propto \frac{1}{\sqrt{(z_2 - z_1)}} \left\{ \frac{(z_2 - z_0)}{\sqrt{1 + (z_2 - z_0)^2}} + \frac{(z_0 - z_1)}{\sqrt{1 + (z_0 - z_1)^2}} \right\} \tag{21}$$

At the transition point we have $z_2 = (z_0 + \delta)$ where δ denotes the half-width of the overlap between the two regions. At this point equation (21) becomes:

$$TSNR \propto \frac{1}{\sqrt{\Delta}} \left\{ \frac{\delta}{\sqrt{1 + \delta^2}} + \frac{\Delta - \delta}{\sqrt{1 + (\Delta - \delta)^2}} \right\} \tag{22}$$

In the limit $\delta \to \Delta/2$ (complete overlap of the two regions) we obtain the result given by equation (19). In the limit $\delta \to 0$ $TSNR \propto \frac{1}{\sqrt{\Delta}} \left\{ \frac{\Delta}{\sqrt{1 + (\Delta)^2}} \right\}$, which is equal to 0.63 for $\Delta = 2.0$.

For $\delta = \Delta/4$ (half overlap as shown in figure (13), the RHS of equation (21) is 0.90 which is very close to the maximum possible value of unity. Thus $\Delta = 2.0$ and half overlap appear to be near optimum for the chosen source and background models.

The example of the previous section was analyzed using 7 overlapping regions that covered all 160 samples. For this example the spectral resolution was reduced to 128 channels and the first 5 PC spectra were used. The samples and the resulting reduced χ^2 values are shown in table 4.

Table 4. Results of multi-region analysis using the ^{137}Cs spectrum for target. The χ^2 values are based on 100 simulation sets.

Region	Starting sample	Ending sample	Average χ^2	Min χ^2	Max χ^2
1	1	41	81.4	11.8	588
2	21	61	90.7	17.7	493
3	41	81	101.9	18.4	676
4	61	101	35.2	5.28	242
5	81	121	1.22	0.84	1.65
6	101	141	1.72	1.00	2.91
7	121	160	17.9	4.28	68.1

For region 5, these results show a slight improvement over the 1-region analysis results in table 2 (χ^2 = 1.62). We were expecting better improvement based on the increased separation of noise and physical variance in the first 5 PC spectra because of the increase in TSNR. Further optimization for multiple region analysis will be considered in future studies.

VI. Detection of Multiple Isotope Sources

In the previous sections the TPCA method was illustrated for detection of sources that were represented by a single spectrum. The same method can be applied to detection of sources composed of multiple isotopes with unknown concentration ratios. Important examples of this are SNM sources with unknown enrichment, age, or source of origin.

To apply the TPCA method it still has to be assumed that all isotopes that make up the target result in the same measured spatial/temporal profile. For this case Eq. (6) and (7) are modified to include multiple target spectra as follows:

$$\sum_{i=1}^{\nu} \beta_i \; T_i(E) \approx \sum_{i=1}^{N'} \alpha_i \; P_i(E) \tag{23}$$

$$\chi^2 = \frac{1}{\left(M_c - N' - [\nu - 1]\right)} \sum_{j=1}^{M_c} \frac{\left[\sum_{i=1}^{\nu} \beta_i \; T_i(E_j) - \sum_{i=1}^{N'} \alpha_i \; P_i(E_j)\right]^2}{\sigma^2(E_j)} \tag{24}$$

where ν is the number of isotopes in the target; $T_i(E)$ is the spectrum for the i-th isotope; and the coefficients, β_i, denote the unknown relative isotopic composition. All other quantities are as defined previously. One of the coefficients, β_i, is arbitrary and can be set to 1 and therefore the number of degrees of freedom is reduced by (ν - 1).

The solution for the coefficients in Eq. (24) is obtained in the normal way by solving the linear system resulting from the minimization of χ^2, that is:

$$\frac{\partial \chi^2}{\partial \alpha_i} = 0 \qquad i = 1, \cdots, N'$$

and

$$\frac{\partial \chi^2}{\partial \beta_i} = 0 \qquad i = 1, \cdots, \nu - 1$$

The above linear system needs to be solved with the constraint that all coefficients, β_i, are positive. This constraint is easily incorporated in the solution by forcing the largest negative coefficient to zero and repeating the solution without the associated spectrum.

Direct measurements can also be used in Eq. (23) as discussed in the previous section depending on the problem being addressed. Implementation and testing of the TPCA method for sources with multiple isotopes will be considered in future work.

V. Summary and Conclusions

In this report we have considered a new spectral analysis method, TPCA, which uses spatial/temporal variations in multiple measurements to test the hypothesis of the presence of a target isotope of interest. This is done without any required knowledge of other background isotopes that might also be present. The only requirement for the method to work properly is that the spatial distribution for the target of interest is different from that for the background sources.

We applied the TPCA method to the problem of detection of a localized source that is embedded in a distributed source in the presence of an ambient background. The measurements were simulated for an RPM-like setup. The method worked very well and detected the presence of the target without any information on the other six clutter isotopes present in the measurements. Also, for a case without the target, the resulting residual clearly indicated absence of the target.

This method is anticipated to complement full spectrum analysis methods such as implemented in GADRAS. It is specifically applicable to cases where multiple measurements are taken and there is an expected difference between the spatial distribution of the target of interest and that for other clutter. In addition to detection of embedded sources, this method is expected to be ideal for search problems where the background is complex and is spatially varying. Similarly we expect the method to work well for RPM applications where the background is spatially and spectrally varying as a result of strong vehicle-induced background suppression.

This report only covered the basic application of the method for the problem of detection of embedded sources and significant additional work is needed to include effects of shielding, optimization of parameters, noise isolation in relation to the derived principal component spectra, and applicable constraints to limit residuals to physically realizable spectra. In addition, further work is required for estimation of target activity, localization, and estimation of detection limits and false positive rates.

Because of the isolation of one or a few target isotopes, this method is well-suited for automated applications. Also, this leads to significantly simpler optimization for effects of shielding and calibration changes since the number of local minima in the optimization processes is expected to be much smaller than for conventional analysis methods because of the smaller number of degrees of freedom.

Appendix A: Description of Generation of Principal Components

Principal Component Analysis (PCA) is a method that involves decomposition of a data covariance or correlation matrix to extract features of a series of measurements in the form of orthogonal vectors. The extracted vectors are ordered according to how dominant the features they represent are in the measured data. The description given here follows the treatment given in reference (3).

Let data matrix $\underline{\underline{\mathbf{D}}}$ represent a set of measurements where each column represents a measured spectrum. The rows represent channel energy, wavelength, time sample, or some other measurement characteristic. For the purposes of our analysis, the measurement data will not be normalized, so that the data contributes directly to the Principal Component vectors (PCs).

The data matrix $\underline{\underline{\mathbf{D}}}$ is made up of (r) rows and (c) columns. The objective is to decompose $\underline{\underline{\mathbf{D}}}$ according to:

$$\underline{\underline{\mathbf{D}}} \approx \underline{\underline{\mathbf{R}}}\,\underline{\underline{\mathbf{C}}}, \tag{A.1}$$

where $\underline{\underline{\mathbf{R}}}$ is (r x n) matrix of factors, $\underline{\underline{\mathbf{C}}}$ is (n x c) matrix of the loadings or contributions to the measurements, and (n) is the number of factors. The factors are the PC vectors.

Given the data matrix $\underline{\underline{\mathbf{D}}}$, one can attempt to find (n), $\underline{\underline{\mathbf{R}}}$, and $\underline{\underline{\mathbf{C}}}$. These can be calculated in multiple ways and are not unique. The PCA procedure is effective because it calculates these quantities in a way that extracts the features in the original data matrix according to their degree of dominance in the data. Consider the matrix $\underline{\underline{\mathbf{Z}}} = \underline{\underline{\mathbf{D}}}\,\underline{\underline{\mathbf{D}}}^{\mathbf{T}}$, which is an (r x r) square matrix:

$$\underline{\underline{\mathbf{Z}}} = \begin{bmatrix} \text{r x c} \\ \text{matrix} \end{bmatrix} \begin{bmatrix} \text{c x r matrix} \end{bmatrix}$$

When the mean measurement is subtracted from the measurements in the data matrix, $\underline{\underline{\mathbf{Z}}}$ is the usual covariance matrix. Otherwise $\underline{\underline{\mathbf{Z}}}$ is a covariance matrix about the origin. Consider the diagonalization process of $\underline{\underline{\mathbf{Z}}}$, i.e. finding its eigenvalues and eigenvectors:

$$\underline{\underline{\mathbf{Z}}}\,\underline{\mathbf{q}}_i = \lambda_i\,\underline{\mathbf{q}}_i \qquad i = 1,\ldots,r \tag{A.2}$$

For now we assume that the number of measurements (c) is large enough (i.e. c > r) so that (r) non-zero eigenvalues and eigenvectors can be calculated. Later this assumption will be relaxed. Let the matrix $\underline{\underline{\mathbf{Q}}}$ be defined by $\underline{\underline{\mathbf{Q}}} = \left[\underline{\mathbf{q}}_1, \underline{\mathbf{q}}_2, ..., \underline{\mathbf{q}}_r \right]$. Thus equation (A.2) can be written as:

$$\underline{\underline{\mathbf{Z}}}\,\underline{\underline{\mathbf{Q}}} = \underline{\underline{\mathbf{Q}}}\,\underline{\underline{\boldsymbol{\lambda}}} \tag{A.3}$$

where $\underline{\underline{\boldsymbol{\lambda}}}$ is a diagonal matrix with elements $\lambda_{ij} = \lambda_i \, \delta_{ij}$. Since the eigenvectors $\underline{\mathbf{q}}_i$ are orthonormal, the matrix $\underline{\underline{\mathbf{Q}}}$ is an orthogonal matrix, that is, $\underline{\underline{\mathbf{Q}}}^{\mathbf{T}} = \underline{\underline{\mathbf{Q}}}^{-1}$. Multiply equation (A.3) by $\underline{\underline{\mathbf{Q}}}^{\mathbf{T}}$:

$$\underline{\underline{\mathbf{Q}}}^{\mathbf{T}}\,\underline{\underline{\mathbf{Z}}}\,\underline{\underline{\mathbf{Q}}} = \underline{\underline{\boldsymbol{\lambda}}}$$

or

$$\underline{\underline{\mathbf{Q}}}^{\mathbf{T}}\,\underline{\underline{\mathbf{D}}}\,\underline{\underline{\mathbf{D}}}^{\mathbf{T}}\,\underline{\underline{\mathbf{Q}}} = \underline{\underline{\boldsymbol{\lambda}}} \tag{A.4}$$

This equation can be separated out as:

$$\underline{\underline{\mathbf{U}}}\,\underline{\underline{\mathbf{U}}}^{\mathbf{T}} = \underline{\underline{\boldsymbol{\lambda}}} \tag{A.5}$$

where $\underline{\underline{\mathbf{U}}}$ is defined by: $\underline{\underline{\mathbf{U}}} = \underline{\underline{\mathbf{Q}}}^{\mathbf{T}}\,\underline{\underline{\mathbf{D}}}$. Multiplying on the left side by the matrix $\underline{\underline{\mathbf{Q}}}$ we obtain:

$$\underline{\underline{\mathbf{D}}} = \underline{\underline{\mathbf{Q}}}\,\underline{\underline{\mathbf{U}}} \tag{A.6}$$

Note that equation (A.6) can be written as an equality only when the product $\underline{\underline{\mathbf{Q}}}\,\underline{\underline{\mathbf{Q}}}^{\mathbf{T}}$ is the identity matrix of size (r) which assumes that (r) eigenvalues and eigenvectors have been determined. From equation (A.1) the following identifications can be made:

$\underline{\underline{\mathbf{R}}} = \underline{\underline{\mathbf{Q}}}$ (r x r) matrix

$\underline{\underline{\mathbf{C}}} = \underline{\underline{\mathbf{U}}}$ (r x c) matrix (n = r)

Thus $\underline{\underline{\mathbf{Q}}}$ is the orthogonal matrix of Principal Component vectors and $\underline{\underline{\mathbf{U}}}$ is the matrix of coefficients for all the measurements. We also have from equation (A.5):

$$\underline{\underline{\boldsymbol{\lambda}}} = \begin{bmatrix} C_{11} \ldots C_{1c} \\ C_{21} \\ \vdots \\ \vdots \\ C_{r1} \ldots C_{rc} \end{bmatrix} \begin{bmatrix} C_{11} \cdots & \\ \vdots & \\ C_{1c} \cdots & \end{bmatrix} \tag{A.7}$$

Expanding this out we get:

$$\lambda_1 = C_{11}^2 + C_{12}^2 + \cdots + C_{1c}^2 \qquad \text{for first PC} \tag{A.8}$$

$$\lambda_2 = C_{21}^2 + C_{22}^2 + \cdots + C_{2c}^2 \qquad \text{for second PC} \tag{A.9}$$

and so on for the other eigenvalues. Thus the first eigenvalue is the sum of the squares of the coefficients for all the measurements for the first principal component vector and so on for the other eigenvalues. Because we assumed that (r) orthonormal eigenvectors are determined, these eigenvectors span the measurement space (i.e. form a complete set) and therefore any measurement vector $\underline{\mathbf{M}}$ in the space can be expressed by the projections on these eigenvectors as follows:

$$\underline{\mathbf{M}} = \sum_{k=1}^{r} \left(\underline{\mathbf{M}} \bullet \underline{\mathbf{q}}_k \right) \underline{\mathbf{q}}_k \tag{A.10}$$

The PCA method is useful for cases when a relatively small number of PC vectors adequately represent measurements of interest. This is indicated by the magnitudes of the eigenvalues as given in Eq. (A.7). For such cases Eq. (A.10) can be truncated to a small number of elements. This is also applicable to cases where the number of measurements is smaller than the dimension of the measurement space (c < r). For this case the maximum possible number of eigenvectors is (c) and the matrix $\underline{\underline{\mathbf{Q}}}$ is no longer a square matrix.

For the numerical generation of the principal components, we used the Jacobi and the Householder transformation methods, both as implemented in Numerical Recipes[(4)]. These Numerical Recipes functions calculate the eigenvalues and eigenvectors of real symmetric matrices and both worked well with very similar results. The Householder transformation method however was found to be considerably faster.

Representing PC Vectors in Terms of the Measurement Vectors:

In the variance estimate discussed in section III of this report, it is required to express the PC vectors as linear combinations of the measurement vectors used to calculate these PC vectors. This representation can be obtained directly from Eq. (A.2) or (A.3) for the i-th eigenvector:

$$\begin{aligned} Q_{k\,i} &= \frac{1}{\lambda_i}\left(\underline{\underline{\mathbf{D}}}\;\underline{\underline{\mathbf{D}}}^{\mathbf{T}}\;\underline{\underline{\mathbf{Q}}}\right)_{k\,i} \\ &= \frac{1}{\lambda_i}\sum_{m=1}^{c} D_{k\,m}\sum_{j=1}^{r} D_{j\,m}\;Q_{j\,i} \end{aligned} \tag{A.11}$$

where $Q_{k\,i}$ is the k-th element of the i-th eigenvector $\underline{\mathbf{q}}_i$. Note that (c) the number of measurements and (r) the measurement dimension are used as defined previously. Writing the same equation in vector form we obtain:

$$\underline{\mathbf{q}}_i = \frac{1}{\lambda_i}\sum_{m=1}^{c}\underline{\mathbf{M}}_m\left(\underline{\mathbf{M}}_m \bullet \underline{\mathbf{q}}_i\right) \tag{A.12}$$

This equation can be verified numerically as a check on the derived PC vectors. We can also write Eq. (A.12) as:

$$\underline{\mathbf{q}}_i = \sum_{m=1}^{c}\alpha_m\;\underline{\mathbf{M}}_m\;,\;\;\alpha_m = \frac{1}{\lambda_i}\left(\underline{\mathbf{M}}_m \bullet \underline{\mathbf{q}}_i\right) \tag{A.13}$$

which provides the needed linear combination expressing the PC vectors in terms of the measurement vectors.

Appendix B: Representation of Signals by Idealized Simple Sources

The simple models of sources in this appendix were used in several previous studies and are included here for completeness. With proper choice of the parameters these models can adequately represent profiles from actual measurements.

Point Source

The simplest possible representation for a source is an isotropic point source. Consider an isotropic point source of strength S_o (units of photons per unit time) placed at the origin of a coordinate system. In this coordinate system, the particle's (photon's) current density (units of photons per unit area per unit time) at radius r is given by

$$\vec{J} = \frac{S_o}{4\pi r^2}\hat{r}\,, \tag{B.1}$$

where $\hat{r}$ is the unit vector along radius r. For a detector of area ΔA with normal unit vector $\hat{n}$, the photon flux through the detector is

$$flux = \frac{S_o}{4\pi r^2}\Delta A\,(\hat{r}\cdot\hat{n})\,. \tag{B.2}$$

The detector area is assumed to be small enough so that only one radial vector needs to be considered. If the detector is oriented along the x-axis (detector in y-z plane, i.e., $\hat{n} = \hat{x}$) and is located at distance r from the source (defined by position vector $\vec{r} = \Delta x\,\hat{x} + \Delta y\,\hat{y} + \Delta z\,\hat{z}$), then the flux through the detector is

$$flux = \frac{S_o}{4\pi r^3}\Delta A\,\Delta x\,, \tag{B.3}$$

where $r = \left(\Delta x^2 + \Delta y^2 + \Delta z^2\right)^{1/2}$. Because the dependence of the flux on z (the direction of vehicle motion) is only through the distance between detector and source along z, the coordinate system can be translated along the z-axis so that the source and detector are at positions z and z_o, respectively. Following this convention, we obtain

$$flux = \frac{S_o\,\Delta A\,\Delta x}{4\pi\left[R_o^{\,2} + (z - z_o)^2\right]^{3/2}}\,, \tag{B.4}$$

where $R_o^{\,2} = \Delta x^2 + \Delta y^2$ is the perpendicular distance from the detector to the z-axis. This can be written as

$$flux = F(z) = A_0\left[\frac{R_0^2}{R_0^2 + (z - z_o)^2}\right]^{3/2}\,, \tag{B.5}$$

where A_0 is the signal amplitude.

Ideal Line Source

We assume a simple line source extending from $(z_0 - \Delta)$ to $(z_0 + \Delta)$ with the same detector configuration as above. Integrating the expression for a point source over this range, we obtain

$$flux \propto \left\{ \frac{z - z_o + \Delta}{\left[R_o{}^2 + (z - z_o + \Delta)^2\right]^{1/2}} - \frac{z - z_o - \Delta}{\left[R_o{}^2 + (z - z_o - \Delta)^2\right]^{1/2}} \right\}$$

or

$$F(z) = \alpha_0 \left\{ \frac{z - z_o + \Delta}{\left[R_o{}^2 + (z - z_o + \Delta)^2\right]^{1/2}} - \frac{z - z_o - \Delta}{\left[R_o{}^2 + (z - z_o - \Delta)^2\right]^{1/2}} \right\}. \tag{B.6}$$

The signal amplitude in this case is given by $F(z = z_0) = \dfrac{2\,\alpha_0\,\Delta}{\left[R_0^2 + \Delta^2\right]^{1/2}} \equiv A_0$.

The radiation signals are given as functions of time and can be translated to *z*-position by using the vehicle speed. By the same token, the above source representations are given in terms of *z*-position and can be changed to time units by dividing by the vehicle speed.

Note that in the limit $\Delta \to 0$, Equation B.6 reduces to the point-source limit. This can be shown by using a Taylor expansion, which gives

$$\begin{aligned}
\lim_{\Delta \to 0} F(z) &\to \alpha_0 \left\{ (z - z_0 + \Delta)\left[\frac{1}{U} - \frac{(z - z_0)\Delta}{U^3}\right] - (z - z_0 - \Delta)\left[\frac{1}{U} + \frac{(z - z_0)\Delta}{U^3}\right] \right\} \\
&\to \alpha_0 \left\{ \frac{2\Delta}{U} - \frac{2\,(z - z_0)^2\,\Delta}{U^3} \right\} \\
&= \frac{2\,\alpha_0\,\Delta}{U}\left[1 - \frac{(z - z_0)^2}{U^2}\right] = \frac{2\,\alpha_0\,\Delta}{U}\,\frac{R_0^2}{U^2}
\end{aligned}$$

where $U = \left[R_0^2 + (z - z_0)^2\right]^{1/2}$. Using the above definition of the amplitude, we obtain the point-source limit:

$$\lim_{\Delta \to 0} F(z) \to 2\left[\frac{A_0}{2\,\Delta} R_0\right]\frac{\Delta\,R_0^2}{U^3} = A_0\left[\frac{R_0^2}{R_0^2 + (z - z_0)^2}\right]^{3/2}.$$

References

(1) Ely, J., Kouzes, R., Schweppe, J., Siciliano, E., Strachan, D., Weier, D.,"The Use of Energy Windowing to Discriminate SNM from NORM in Radiation Portal Monitors," Pacific Northwest National Laboratory SA 44680, *Nuclear Instruments and Methods in Physics Research A*, 560: 373-387, 2006.

(2) Burr, T., Gattiker, J. R., Myers, K. Tompkins, G. "Alarm criteria in radiation portal monitoring" *Applied Radiat. Isotopes* (2007)

(3) I. R. Shokair and D. Cohen, "Detecting Embedded Localized Radiation Sources by Using Radiation Portal Monitor Data", Sandia National Laboratories report SAND2008-3469, October 2008.

(4) I. R. Shokair and T. A. Reichardt, "Targeted Detection Using Fusion of Spectral and Spatial/Temporal Information", Sandia National Laboratories report SAND2011-xxxx, September 2011.

(5) D. J. Mitchell, H. M. Sanger, and K. W. Marlow, "Gamma-Ray Response Functions for Scintillation and Semiconductor Detectors", *J. Nuc. Inst. And Methods in Physics Research A276* (1989), 547-556.

(6) D. R. Waymire and D. J. Mitchell, "GADRASw User Manual", updated November 2009.

(7) D. J. Mitchell, "Variance Estimation for Analysis of Radiation Measurements", Sandia National Laboratories report SAND2008-2302, April 2008.

(8) E. R. Malinowski and D. G. Howery, "Factor Analysis in Chemistry", Krieger Publishing Company, Malabar, Florida, 1989.

Distribution

1 Thomas L. Burr and Paul Flecher
Los Alamos National Laboratory
MS F600
PO Box 1663
Los Alamos, NM 87545

1 Robert Runkle and Mark Tardiff – James Ely, David Pfund
Pacific Northwest National Laboratory
MS P7-80
PO Box 999
Richland WA 99352

1

1	MS 1316	Mark Daniel Rintoul, 1465
1	MS 0782	Dean J. Mitchell, 6633
1	MS 0782	George Lasche, 6633
1	MS 9004	Peter B. Davies, 8100
1	MS 9004	Howard H. Hirano, 8110
1	MS 9003	Jason C. Reinhardt, 8112
1	MS 9003	Gary W. Richter, 8112
1	MS 9003	Mathew Sumner, 8112
1	MS 9003	Janson Wu, 8112
1	MS 9004	Duane L. Lindner, 8120
1	MS 9056	Thomas A. Reichardt, 8128
1	MS 9104	Willard R. Bolton, 8123
5	MS 9104	Isaac R. Shokair, 8123
1	MS 9104	Larry R. Thorne, 8123
1	MS 9104	Tim P. Tooman, 8123
1	MS 9004	James C. Lund, 8130
1	MS 9402	John E. M. Goldsmith, 8131
1	MS 9402	Arlyn J. Antolak, 8131
1	MS 9402	Kristin L. Hertz, 8131
1	MS 9402	Nathan R. Hilton, 8131
1	MS 9402	William C. Johnson, 8131
1	MS 9402	Christopher L. Kunz, 8131
1	MS 9104	Jay R. Spingarn, 8131
1	MS 9406	Erik Brubaker, 8132
1	MS 9406	Wondwosen Mengesha, 8132
1	MS 9154	William P. Ballard, 8200
1	MS 9159	Noel M. Nachtigal, 8958

1 MS 0899 Technical Library, 9536